# Comparing Pythia Output with Data

A Preliminary Look - Version IV

*Alex R. Dzierba*

## Introduction

This is a preliminary look at Monte Carlo data simulated by Pythia comparing it to published data[1]. I am using Pythia parameters as tuned by Eugene Chudakov and Elke Aschenauer and as passed on to me by David Lawrence. I generated $10^5$ events with $E_\gamma = 9$ GeV. This is a work in progress and this note will be updated.

## Distribution in particle types

The distribution in final state particle types, using the GEANT-based numbering scheme is shown in Figure 1. Note that the vertical scale is logarithmic. This distribution is repeated in Figure 2(a) but now with a linear scale along the distribution in numbers of particles, numbers of charged particles and numbers of photons (in Figure 2(b) through (d) respectively).

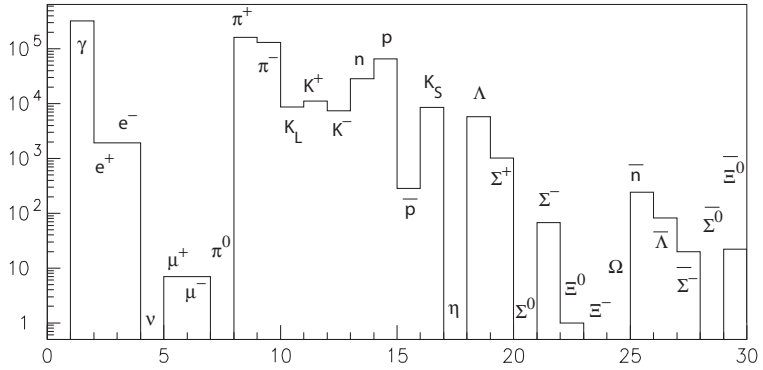


Figure 1: Distribution of types of final state particles from the Pythia simulation.

## Distribution among topologies

Cross sections for various topologies for an incident photon energy of 9 GeV are summarized in Table 1. Comparison of Pythia cross section measurements and measured cross sections for specific exclusive 3-prong and 5-prong reactions are shown in Table 2. Pythia cross section estimates are based on a total photoproduction cross section of 124 $\mu$b. Some ratios of cross sections are shown in Table 3.

[1] Cross sections at GlueX energies are summarized in A. Dzierba, GlueX-doc-825.

Table 1: Topological Photoproduction Cross Sections at 9 GeV from Pythia and from bubble chamber data (ref: H. Bingham *et al., Phy. Rev.* **D8** (1973) 1277). The Pythia cross section estimates assume a total photoproduction cross section of 124 $\mu$b. The errors on the Pythia estimates are statistical.

| Topology | Pythia Estimates ($\mu$b) | Data ($\mu$b) |
|---|---|---|
| 1-prong | $8.79 \pm 0.02$ | $6.9 \pm 0.9$ |
| 3-prong | $63.5 \pm 0.09$ | $51.7 \pm 1.2$ |
| 5-prong | $42.7 \pm 0.2$ | $27.6 \pm 0.7$ |
| 7-prong | $7.3 \pm 0.1$ | $5.5 \pm 0.2$ |
| 9-prong | $0.3 \pm 0.1$ | $0.5 \pm 0.06$ |

Table 2: Photoproduction reaction cross sections at 9 GeV from Pythia and from bubble chamber data (ref: H. Bingham *et al., Phy. Rev.* **D8** (1973) 1277). The Pythia cross section estimates assume a total photoproduction cross section of 124 $\mu$b. The errors on the Pythia estimates are statistical.

| Reaction | Pythia Estimates ($\mu$b) | Data ($\mu$b) |
|---|---|---|
| | $\gamma p \to 3$ prongs | |
| $\gamma p \to p\pi^+\pi^-$ | $13.6 \pm 0.13$ | $14.7 \pm 0.6$ |
| $\gamma p \to pK^+K^-$ | $0.41 \pm 0.02$ | $0.58 \pm 0.05$ |
| $\gamma p \to p\bar{p}p$ | $0.04 \pm 0.01$ | $0.09 \pm 0.02$ |
| $\gamma p \to p\pi^+\pi^-\pi^0$ | $5.8 \pm 0.1$ | $7.5 \pm 0.8$ |
| $\gamma p \to n2\pi^+\pi^-$ | $1.4 \pm 0.04$ | $3.2 \pm 0.7$ |
| With multi-neutrals | $42.3 \pm 0.3$ | $38.0 \pm 1.9$ |
| | $\gamma p \to 5$ prongs | |
| $\gamma p \to p2\pi^+2\pi^-$ | $2.9 \pm 0.06$ | $4.1 \pm 0.2$ |
| $\gamma p \to pK^+K^-\pi^+\pi^-$ | $0.51 \pm 0.03$ | $0.46 \pm 0.08$ |
| $\gamma p \to p2\pi^+2\pi^-\pi^0$ | $8.12 \pm 0.1$ | $6.7 \pm 1.0$ |
| $\gamma p \to n3\pi^+2\pi^-$ | $0.8 \pm .3$ | $1.8 \pm 1.9$ |
| With multi-neutrals | $30.4 \pm 0.2$ | $21.1 \pm 1.7$ |

Table 3: Ratios of cross sections for various reactions for an incident photon energy of 9 GeV.

| Ratio | Pythia (%) | Data (%) |
|---|---|---|
| $\sigma(\pi^+\pi^-p)/\sigma(3\text{-prong})$ | 21 | $23 \pm 1$ |
| $\sigma(\pi^+\pi^-\pi^0p)/\sigma(3\text{-prong})$ | 9 | $11 \pm 1$ |
| $\sigma(\omega p)/\sigma(\pi^+\pi^-\pi^0p)$ | 24 | $25 \pm 4$ |

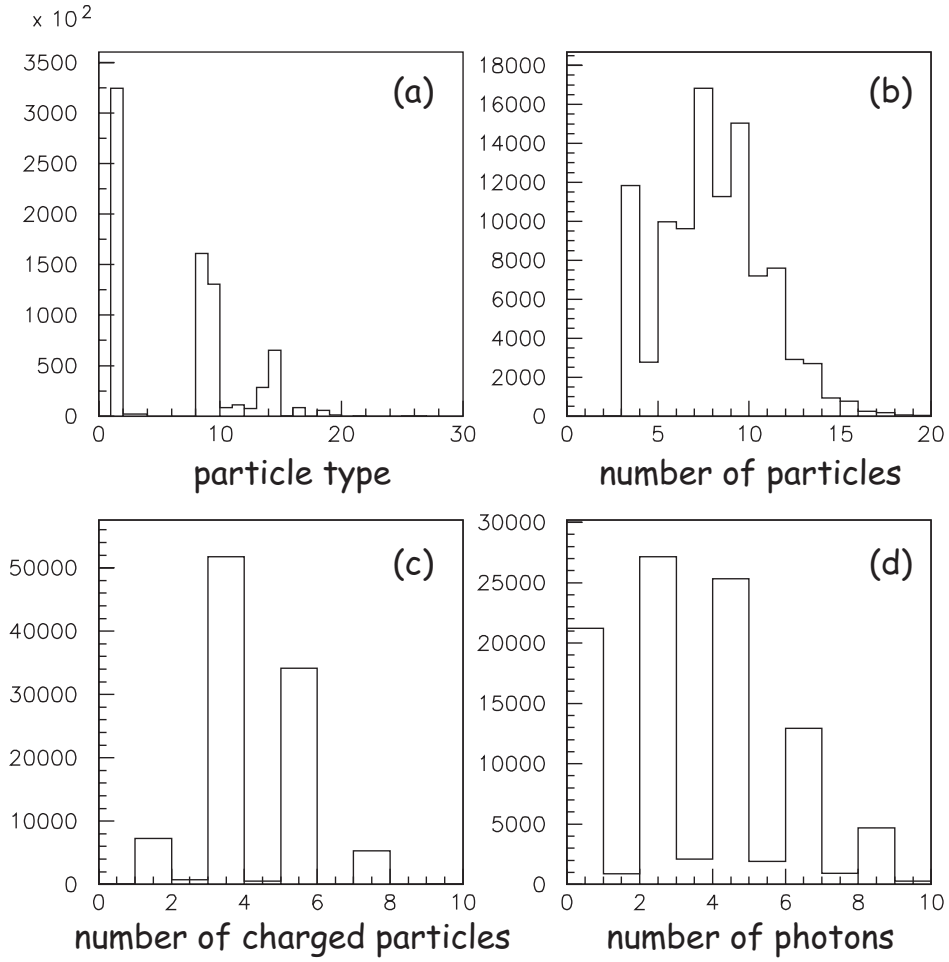


Figure 2: (a) Same as Figure 1 but with a linear vertical scale; (b) Distribution in the number of particles; (c) Distributions of number of charged particles; and (d) Distribution in the number of photons.

**Three-prong sample**

**No neutrals:** Distributions for Pythia data corresponding to $\gamma p \to \pi^+\pi^- p$ are shown in Figure 3. At 9 GeV $\gamma p \to \rho^0 p$ accounts for 92% of $\gamma p \to \pi^+\pi^- p$ for data, consistent with Pythia simulations. The $2\pi$ effective mass distribution is shown in Figure 3(a) and the $\pi^+ p$ and $\pi^- p$ effective mass distributions are shown in Figures 3(b) and (c). For the $|t|$ distribution (Figure 3(d)), a fit to $dN/d|t| \propto e^{-a|t|}$ yields $a = 7.4 \pm 0.8$ GeV$^{-2}$ for the Pythia data compared to published data for which $a = 6.5 \pm 0.5$ GeV$^{-2}$.

Figure 4 shows (a) the $K^+K^- p$ effective mass distribution showing the $\phi$; (b) distribution in momentum transfer squared from the incident photon to the $2K$ system. The exponential fit yields a slope parameter of $5.5 \pm 0.5$ GeV$^{-2}$. For data, the slope parameter at 9 GeV is $4.8 \pm 0.7$ GeV$^{-2}$.

**With a single $\pi^0$:** Distributions for Pythia data corresponding to $\gamma p \to \pi^+\pi^-\pi^0 p$ are shown in Figure 5. Figure 5(a) shows the $\pi^+\pi^-\pi^0$ effective mass distribution with the $\omega$ clearly seen. Figure 5(b) shows the $2\pi$ effective mass distribution for three possible combinations – the $\rho$ is clearly seen and the lower peak is due to the $\omega$ decays. Figure 5(c) shows the $\pi p$ effective mass distribution for three possible combinations – the $\Delta$ is clearly seen. Published data at 9 GeV yield cross sections for $\omega p$, $\rho^-\Delta^{++}$, $\rho^0\Delta^+$ and $\rho^+\Delta^0$ of

$1.9 \pm 0.3$ $\mu$b, $1.1 \pm 0.2$ $\mu$b, $0.3 \pm 0.2$ $\mu$b and $0.2 \pm 0.2$ $\mu$b respectively. Pythia clearly accounts for baryon resonance production. Figure 5(d)Distribution in momentum transfer squared from the incident photon to the $3\pi$ system.

**With a recoil neutron:** Distributions for Pythia data corresponding to $\gamma p \to 2\pi^+\pi^- n$ at 9 GeV are shown in Figure 6. Figure 6(a) shows the $\pi^+\pi^+$ effective mass distribution. Figure 6(b) shows the $\pi^+\pi^-$ effective mass distribution – with a $\rho^0$. Figure 6(c) shows the $3\pi$ effective mass and Figure 6(d) shows the $\pi^+ n$ and $\pi^- n$ effective mass distributions.

**Multi-neutrals:** Distributions for Pythia data corresponding to $\gamma p \to 3$ prongs at 9 GeV are shown in Figure 7. Figures 7(a) and (b) show the distribution in particle type and the number of photons respectively. Figures 7(c) and (d) show the missing mass recoiling against the three charged particles. Figures 7(d) missing mass distribution for the lower masses and with a logarithmic scale. The peak at zero mass are $\pi^-\pi^+ p$ events. Peaks corresponding to recoil $\pi^0$, $K_S$, $\eta$ and neutron are also seen.

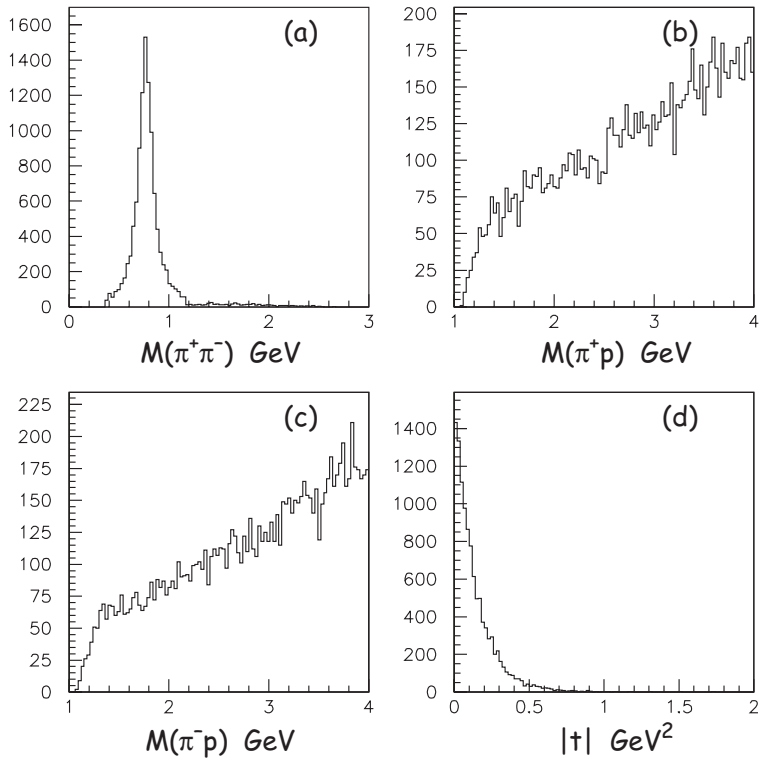


Figure 3: Distributions for Pythia data corresponding to $\gamma p \to \pi^+\pi^- p$ at 9 GeV. (a) The $\pi^+\pi^-$ effective mass distribution showing the $\rho^0$; (b) and (c) The $\pi^+ p$ and $\pi^- p$ effective mass distributions; (d) Distribution in momentum transfer squared from the incident photon to the $2\pi$ system.

**Three-prong sample**

$2\pi^+2\pi^- p$**:** Distributions for Pythia data corresponding to $\gamma p \to 2\pi^+2\pi^- p$ at 9 GeV are shown in Figure 8. Figure 8(a) shows the $\pi^+\pi^+$ and $\pi^-\pi^-$ effective mass distributions. Figure 8(b) shows the $\pi^+\pi^-$ effective mass distribution. Figure 8(c) shows the $2\pi^+2\pi^-$ effective mass distribution and Figure 8(d) shows the $\pi^+ p$

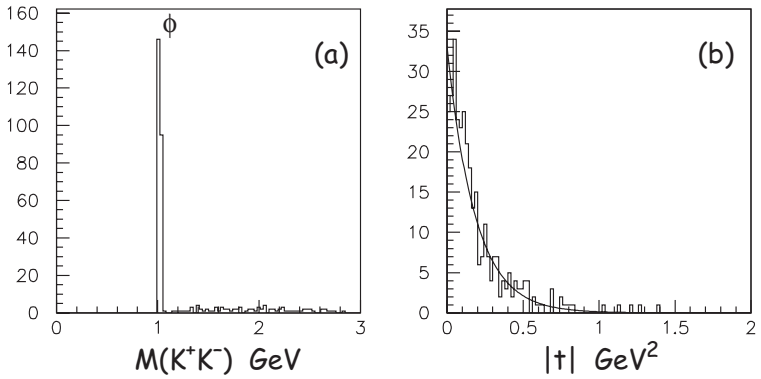


Figure 4: Distributions for Pythia data corresponding to $\gamma p \to K^+K^-p$ at 9 GeV. (a) The $K^+K^-p$ effective mass distribution showing the $\phi$; (b) Distribution in momentum transfer squared from the incident photon to the $2K$ system. The exponential fit yields a slope parameter of $5.5 \pm 0.5$ GeV$^{-2}$.

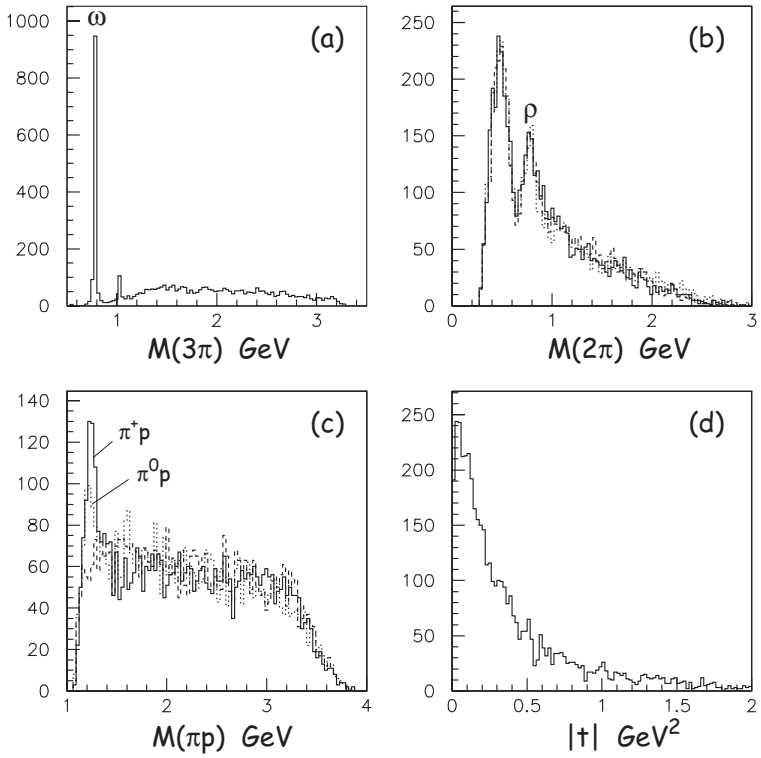


Figure 5: Distributions for Pythia data corresponding to $\gamma p \to \pi^+\pi^-\pi^0 p$ at 9 GeV. (a) The $\pi^+\pi^-\pi^0$ effective mass distribution showing the $\omega$; (b) The $2\pi$ effective mass distribution for three possible combinations – the $\rho$ is clearly seen; (c) The $\pi p$ effective mass distribution for three possible combinations – the $\Delta$ is clearly seen; (d) Distribution in momentum transfer squared from the incident photon to the $3\pi$ system.

and $\pi^- p$ effective mass distributions. The $\rho$ is absent in the $\pi^+\pi^-$ mass distribution. There is a $\Delta^{++}(1236)$ in the $\pi^+ p$ mass distribution.

**$K^+K^-\pi^+\pi^-p$:** Distributions for Pythia data corresponding to $\gamma p \to K^+K^-\pi^+\pi^-p$ at 9 GeV are shown in Figure 9. Figure 9(a) shows the $\pi^+\pi^-$ effective mass distribution with a $\rho$ present. Figure 9(b) shows

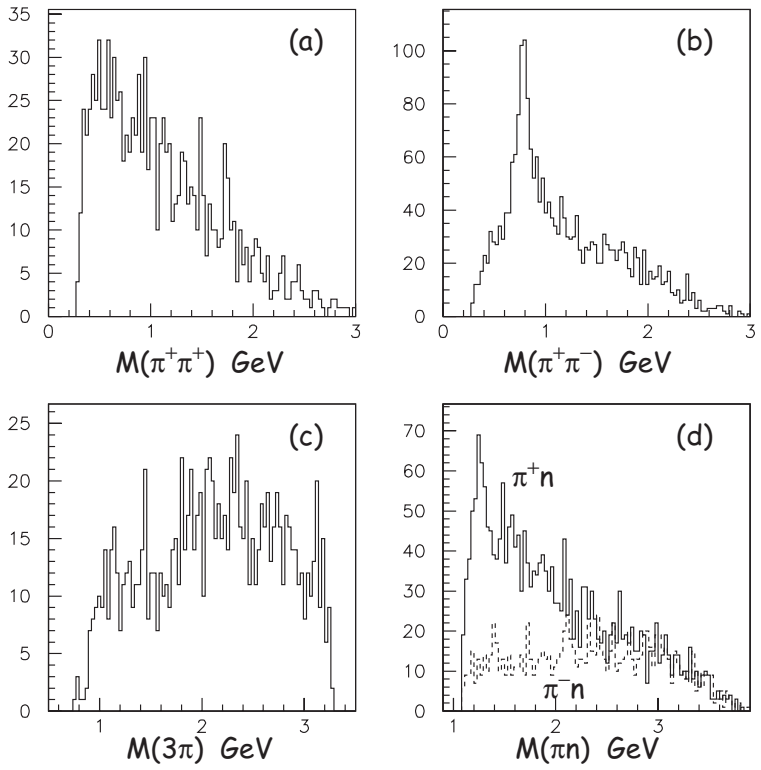


Figure 6: Distributions for Pythia data corresponding to $\gamma p \to 2\pi^+\pi^- n$ at 9 GeV. (a) $\pi^+\pi^+$ effective mass distribution; (b) $\pi^+\pi^-$ effective mass distribution; (c) $2\pi^+\pi^-$ effective mass distribution; and (d) $\pi^+ n$ and $\pi^- n$ effective mass distributions.

the $K^+K^-$ effective mass distribution with a $\phi$ present. Figure 9(c) shows the $K^+\pi^-$, $K^-\pi^+$, $K^+\pi^+$, and $K^-\pi^-$ effective mass distributions. A $K^*(890)$ appears in the $(K\pi)^0$ distributions while the doubly charged $K\pi$ systems show no structure. Figure 9(d) shows the $KK\pi\pi$ effective mass distribution.

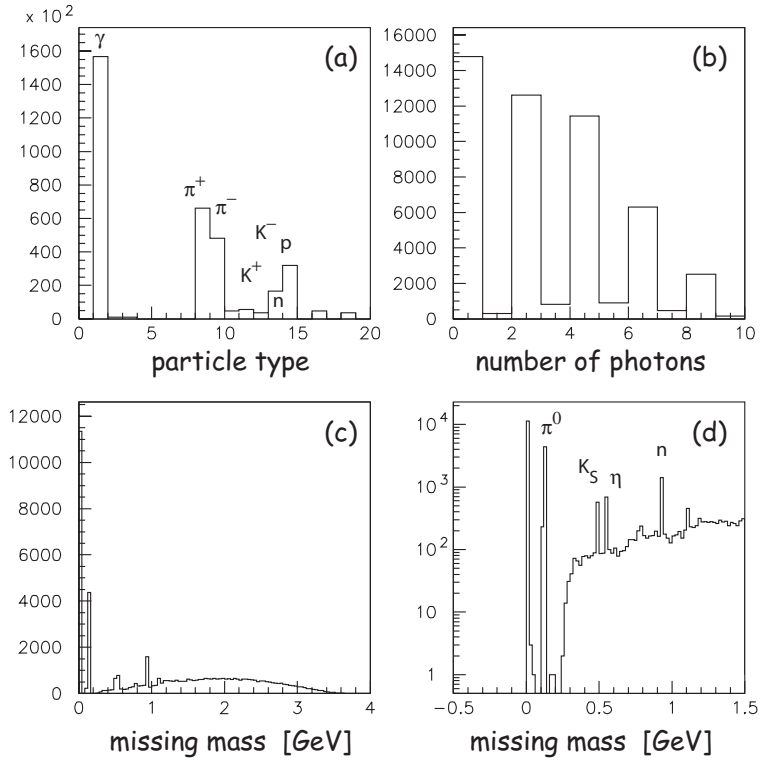


Figure 7: Distributions for Pythia data corresponding to $\gamma p \to 3$ prongs at 9 GeV. (a) Distribution in particle type; (b) Distribution in number of photons; (c) Missing mass recoiling against the three charged particles; (d) Missing mass distribution shown for the lower masses and with a logarithmic scale. The peak at zero mass are $\pi^-\pi^+p$ events. Peaks corresponding to recoil $\pi^0$, $K_S$, $\eta$ and neutron are also seen.

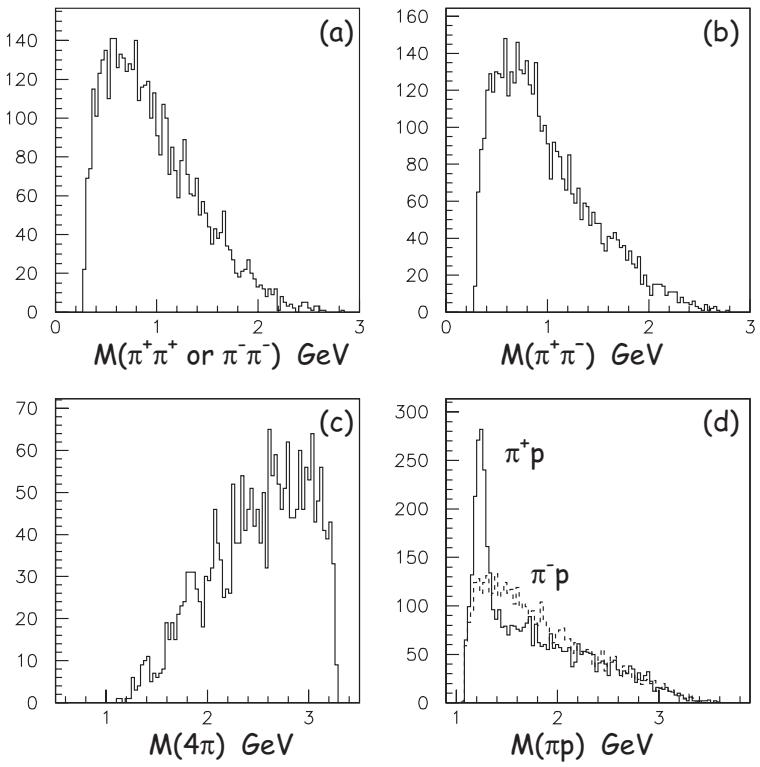


Figure 8: Distributions for Pythia data corresponding to $\gamma p \to 2\pi^+ 2\pi^- p$ at 9 GeV. (a) $\pi^+\pi^+$ and $\pi^-\pi^-$ effective mass distribution; (b) $\pi^+\pi^-$ effective mass distribution; (c) $2\pi^+2\pi^-$ effective mass distribution; and (d) $\pi^+ p$ and $\pi^- p$ effective mass distributions.

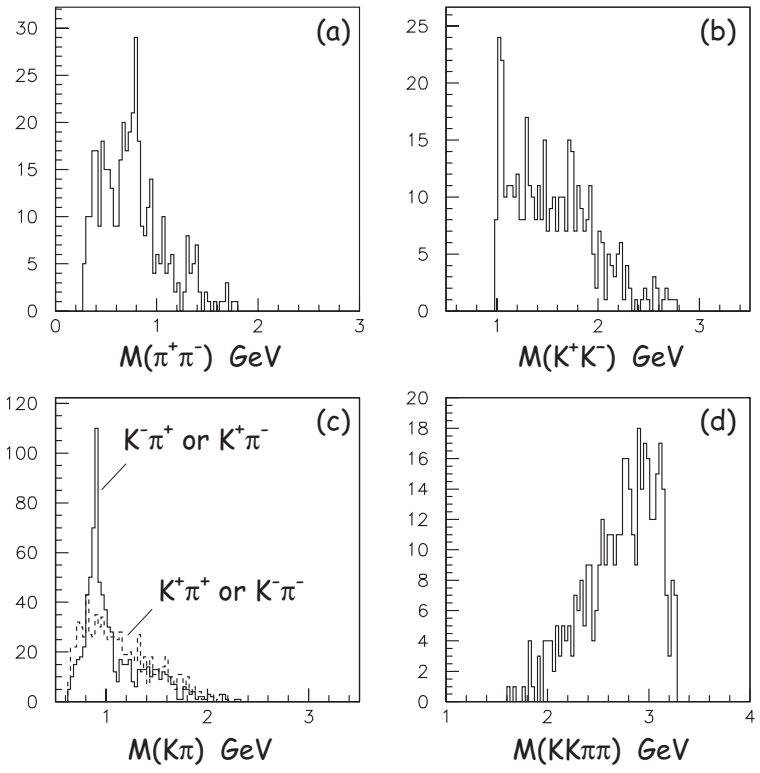


Figure 9: Distributions for Pythia data corresponding to $\gamma p \to K^+K^-\pi^+\pi^-p$ at 9 GeV. (a) $\pi^+\pi^-$ effective mass distribution; (b) $K^+K^-$ effective mass distribution; (c) $K^+\pi^-$, $K^-\pi^+$, $K^+\pi^+$, and $K^-\pi^-$ effective mass distributions; and (d) $KK\pi\pi$ effective mass distribution.